Wiley
Journal of Engineering
Volume 2024, Article ID 2754956, 13 pages
https://doi.org/10.1155/je/2754956

WILEY

Research Article

Numerical Simulation Analysis of a Crude Oil Droplet's Motion Through a Stagnant Aqueous Phase

Abouther Al-Shimmery,[1] **Ali Al-Azzawi**,[1] **Mudhaffar Yacoub Hussein**,[1] **Ahmed Alshara**,[2] **and Mohammed Razzaq Mohammed**[1]

[1]*Department of Chemical Engineering, College of Engineering, University of Misan, Amarah, Iraq*
[2]*Department of Mechanical Engineering, College of Engineering, University of Misan, Amarah, Iraq*

Correspondence should be addressed to Ahmed Alshara; dr.ahmed_alshara@uomisan.edu.iq

Received 20 May 2024; Accepted 2 December 2024

Academic Editor: Hans Kristianto

In this study, computational fluid dynamics (CFDs) simulation analysis was used to predict the dynamic of crude oil droplets in an American Petroleum Institute (API) oil–water separator unit. To mimic the whole separation process (i.e., the oil droplets rising movement) in the API oil–water separator unit, a single oil droplet rising in a stagnant water column has been used. Three main factors were investigated, namely, crude oil specifications (in terms of specific gravity [S.G.] and viscosity), radius of the oil droplet and the position of the oil droplet. The rising velocity of the droplet of the crude oil was characterized in terms of terminal velocity and the centre of the gravity. Generally, the CFD (COMSOL Multiphysics software) analysis succeeded to visualize the hypothetical bath of the crude oil droplet. The results illustrated that the rising velocity increased with decreasing the S.G. and inversely decreased with increasing the viscosity of the crude oil. In addition, the increase in the crude oil droplet diameter had a direct effect on the increasing of the rising velocity. Moreover, it was found that the terminal velocity increased with decreasing the water column over the oil droplet.

Keywords: API separator; CFD simulation; COMSOL multiphysics; level set method

1. Introduction

The petroleum industry is well-known as a water-consuming area due to the considerable volumes of water adopted, the wastewater generated during the production as well as the refining processes. Among the most dominant environmental pollutants is the produced water (i.e., oily wastewater) [1], which is defined as water contaminated with hydrocarbons. Produced water or oily wastewater can be classified into different categories based on the nature of the oil contamination: free, dispersed, emulsified and dissolved oil [2, 3].

The free oil and dispersed oil (i.e., which is found in water as droplets ranging in size from small millimetres-sized droplets to larger droplets [2]) can be easily separated from the continuous phase (i.e., water) via gravity driven-based process. This technique depends on the immiscibility as well as the density differences of continues and dispersed phases (i.e., water–oil). This type of separation can take place either in a stationary or flowing state, after introducing the liquid mixture into the separator, a gravity difference is generated due to the difference in liquids densities. Consequently, the heavier liquid phase settles under the influence of gravity. The American Petroleum Institute (API) oil–water separator (Figure 1(a)), also known as a gravity separator, is a device which is designed to separate oil and light fractions that have a lower density than water from the produced water generated at the wellhead [4] and other industries such as petrochemicals, natural gas, refineries and chemical engineering processes. The main criteria that are used to design API depend on the principle of the Stokes law [5] to define the rising velocity of the oil droplet based on the gravity and the volume of the oil droplet.

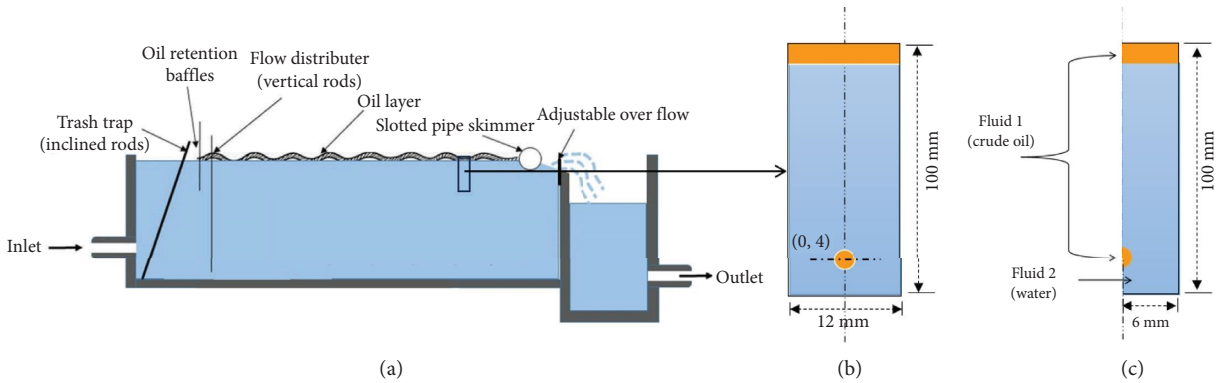

FIGURE 1: Schematic diagram of (a) an API separator, (b) the crude oil droplet rising in water column and (c) a two-dimensional axi-symmetric domain.

The knowledge of dynamic behaviour of crude oil droplet through an immiscible aqueous phase is necessary in crude oil production process, where the crude oil and water are produced and transported together. This in turn leads to enhance and generate the crude oil water emulsions. Therefore, liquid–liquid separation process, including dispersed phase in continues phase (i.e., crude oil droplets in water) needs more attention to understand the main parameters that enhance and accelerate especially demulsification process of oil in water emulsion and the gravity-based separation process. For a spherical body (i.e., crude oil droplet), rising in a continuous phase involves three significant forces which have a direct influence on the dynamic moving of the oil droplet. They are weight, buoyancy, and drag forces. Beginning with the weight force, it is notable that it acts vertically downwards due to the gravity. It can be expressed as the following:

$$F_W = mg, \tag{1}$$

where F_W is the weight force (N), m is the body mass (kg), and g is the acceleration due to gravity (m/s^2).

In counteraction to the weight force, the buoyancy force is acting in an upward direction. This force can be represented by the following equation:

$$F_B = \rho_f V_d g, \tag{2}$$

where F_B is the buoyancy force (N), ρ_f is the fluid density (kg/m^3), V_d is the volume of the immersed body (m^3), and g is the acceleration due to gravity (m/s^2).

Lastly, the drag force (i.e., resisting force) operates in the direction opposite to the body's motion. The magnitude of this force depends on several factors that include size, velocity, shape and fluid properties. It can be described by the following equation:

$$F_D = \frac{1}{2} C_D \rho_f U^2 A, \tag{3}$$

where C_D is the drag coefficient, which is a function of the Reynolds number (Re), ρ_f is the density of the surrounding fluid medium (kg/m^3), U is the velocity of the droplet (m/s), and A represents the effective cross-sectional area of the droplet (m^2).

In the equilibrium state, where the velocity of the droplet remains constant over time (i.e., the terminal velocity), the weight and drag forces will eventually balance out the buoyancy force. This dynamic balance can mathematically be expressed by the following equations:

$$F_W + F_D = F_B, \tag{4}$$

$$\rho_d V_d g + \frac{1}{2} C_D \rho_f U^2 A = \rho_f V_d g. \tag{5}$$

Rearranging equation (2) leads to the following equation:

$$U = \sqrt{\left(\frac{4\left(\rho_f - \rho_d\right) g D_d}{3 C_D \rho_f} \right)}. \tag{6}$$

At low Reynold's number, the drag coefficient can be calculated using the following equation:

$$C_D = \frac{16}{Re}. \tag{7}$$

In the last few decades, a substantial number of experimental investigations and simulations have been undertaken to examine the fluid dynamics of particles, bubbles and droplets in a stagnant liquid [6]. However, there are a few experimental and simulation studies deal with a single crude oil droplet and they can be classified into several categories relying on the type of the chemical additive to the continuous phase. This includes the study of the adding surfactant [7–9], salt concentration and different pH levels [10] on the terminal velocity, shaping deformation processes of a droplet [8, 11, 12].

For instance, Rao et al. [7] examined the impact of sodium dodecyl sulphate (SDS) surfactant on the movement of a single crude oil droplet rising in still water. Experiments involved releasing oil droplets of varying sizes (0.3–0.85 cm) through different nozzles, while varying SDS concentrations (0–750 ppm) in water. The presence of SDS caused a reduction in interfacial tension, resulting in smaller droplets at the nozzle and reduced rise velocities. In addition, Al-Matroushi and Ghannam [11] investigated the flow behaviour of crude oil droplets (with a volume range of 5–70 μL) at

low Reynold's numbers within Newtonian aqueous solutions. The results showed that the dynamic and steady shape deformations of the crude oil droplets were affected by two factors: the viscosity of the continuous phase and the presence of a surfactant, which influences the surface tension of the crude oil droplets. Moreover, Zameek et al. [10] studied the effects of pH and salinity of the continuous phase on the terminal velocity of a droplet heavy crude oil in a static aqueous solution. They found that there was an increase in crude oil droplet terminal velocity with increasing diameter, salt concentration and pH levels. Gao et al. [9] numerically examined the impact of adding chemical dispersant on crude oil rising velocity in a column of water. The findings illustrated that the rising velocity of the oil droplet decreased by 23.4% from the rising velocity without any chemical dispersant. Moreover, Rao et al. [7] curried out an experimental and numerical study to explore the effect of surfactant on the shape and dynamic moving of the oil droplet in a column of water. It was found that at low surfactant concentrations, smaller droplets moved in a straight line. Meanwhile, larger droplets and those in medium with high surfactant concentrations followed a zigzag trajectory.

Besides, Gopalan and Katz [12] studied the oil droplet deformation process with surfactant under isotropic turbulent flow. The results highlighted that multiple, long oil threads were observed behind the oil droplets. Another study was conducted by Laurent Aprin [8], who investigated the effect of the different concentrations of chemical dispersant on the shape deformation processes of the oil droplets. The findings indicated that the volume of the oil droplet decreased by increasing the concentration of the surfactant.

Aforementioned studies examined many parameters that have a direct effect on the terminal velocity that was related to the properties of the continuous phase such as chemical surfactant, viscosity, density and salinity concentration.

However, many parameters, which play a vital role in the process of oil–water separation or, in other words, which accelerate the oil droplet rising velocity, are still need to be investigated. They include the crude oil properties (i.e., specific gravity [S.G.] and viscosity), water level above the oil droplet and droplet diameter of dispersed phase. Therefore, this study seeks to clarify, in more details, the correlation between the rising velocity of the crude oil droplet and these parameters using CFD simulation analysis (COMSOL Multiphysics).

2. CFD Modelling

2.1. Governing Equations. In order to understand the movement of the two-phase interface, a common approach is to employ numerical simulations that involve capturing the interface between the two phases. Two popular methods for this purpose are the volume of fluid (VOF) method and the level set (LS) method [13]. In this study, the LS method was utilized to track the liquid–liquid interface and examine the oil motion. The LS method is a valuable technique that allows for the representation of moving interfaces or boundaries using a fixed mesh. It is particularly useful in situations where the computational domain can be divided into two separate domains by an interface. In addition, each of these domains has the flexibility to consist of multiple parts [8].

The Navier–Stokes and continuity equations essentially govern the unsteady motion of an oil droplet in a stagnant water column. The equations can be written as follows:

$$\rho\left(\left(\frac{\partial u}{\partial t}\right)+u\cdot\nabla u\right)=\nabla\cdot\left[-pI+\mu\left(\nabla u+\nabla u^{T}\right)\right]+F, \tag{8}$$

$$\rho\nabla\cdot(u)=0, \tag{9}$$

where u is the velocity field, p is the pressure field, ρ is the fluid density, μ is the fluid dynamic viscosity, I is the identity matrix, and T stands for matrix transpose. The dominant forces (F) that govern the flow of liquid–liquid two phase are the surface tension force and the gravity force.

The motion of the oil droplet interface was solved via the LS method (see equation (10)).

$$\left(\frac{\partial\phi}{\partial t}\right)+\nabla.(\boldsymbol{u}\,\phi)=\gamma\nabla.\left(\varepsilon\nabla\phi-\phi(1-\phi)\left(\frac{\nabla\phi}{|\nabla\phi|}\right)\right), \tag{10}$$

where ε is the interface thickness (m) and γ is the reinitialization factor

In COMSOL Multiphysics, the LS function (ϕ) is a step function that smoothly transitions from zero to one across an interface. This interface was precisely defined by the 0.5 isocontour, of ϕ. The value of ϕ is zero in one domain and one in another. In addition, the density and viscosity of each phase can be defined via the LS function as follows:

$$\rho=\rho_o+(\rho_w-\rho_o)\phi, \tag{11}$$

$$\mu=\mu_o+(\mu_w-\mu_o)\phi, \tag{12}$$

where ρ_o is the density of crude oil (kg/m^3), ρ_w is the density of water (kg/m^3), μ_o is the viscosity of crude oil (Pa.s) and μ_w is the viscosity of water (Pa.s).

The surface tension force (F_{st}), which is a surface force, can be defined using the following equation:

$$F_{st}=\sigma\kappa\delta n, \tag{13}$$

where σ is the surface tension, κ is the surface curvature, δ is the Dirac function, and n is the unit normal vector to the surface.

However, during the computation, the surface tension force was converted to a volume force and it can be written in the following equation:

$$F_{st}=\sigma\kappa\delta n=\sigma\kappa(\phi)\nabla\phi, \tag{14}$$

and

$$n=\left(\frac{\nabla\phi}{\|\nabla\phi\|}\right), \tag{15}$$

$$\kappa(\phi)=-\nabla\cdot n. \tag{16}$$

Table 1: Properties of the crude oil from different crude oil's field [15].

Properties	Noor	Bazergan	Faqa 1	Faqa 2	Halfaya	Abu-Gharb
Specific gravity at 20°C	0.879	0.890	0.905	0.884	0.913	0.858
Kinematics viscosity cSt at 20°C	40.1	45	33.5	33.6	44	39

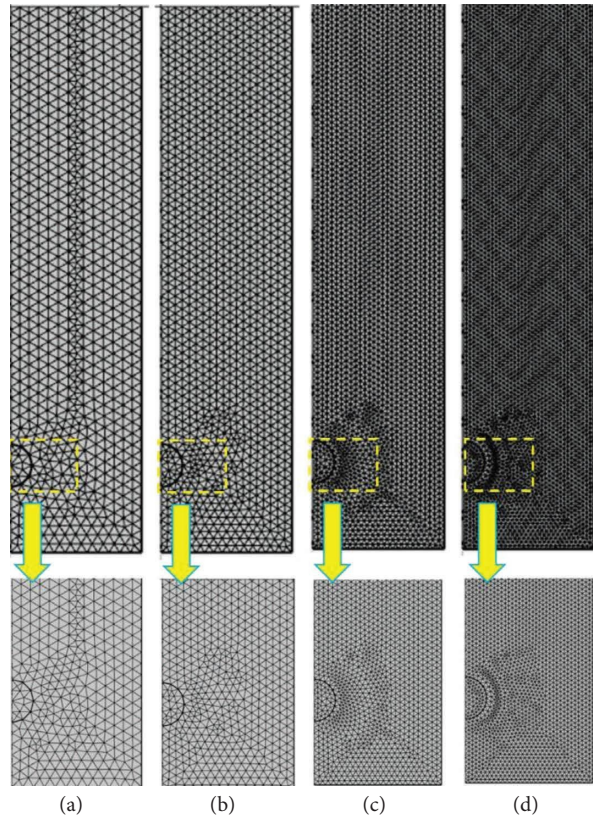

Figure 2: Grid models with different mesh resolutions: (a) coarser, (b) coarse, (c) normal and (d) fine.

Table 2: Statistics characteristics of different types of meshes.

	Coarser	Coarse	Normal	Fine
Number of elements	5827	9568	21,058	34,546
Minimum element quality	0.5651	0.601	0.525	0.6527
Average element quality	0.9283	0.939	0.9504	0.9527
Element area ratio	0.2542	0.2602	0.2663	0.1716
Mesh area (mm^2)	600	600	600	600

2.2. The Problem Description and the CFD Procedure. To represent the whole separation process in API separator (i.e., the oil droplets rising in water), a small part (100 mm (96 mm height of water + 4 mm represent the oily layer), 12 mm) can be taken to setup the computational domain (Figure 1(b)). As a result of the symmetry around the vertical axis, a two-dimensional axisymmetric problem was employed to solve the time-dependent of the governing equations for fluid flow, as illustrated in Figure 1(c) (the rising bubble model, as the closest model, was used to build our model [14]).

The following assumptions were used: the no-slip wall on the side of the domain, and a pressure outlet at the top of the domain were used as boundary conditions. The oil droplet with 2 mm diameter initiated its upward movement from the initial coordinates (0, 4 mm), as depicted within Figure 1(c), and a zero-velocity field within the domain were used as initial conditions. The simulation was used to calculate the steady velocity of the oil droplet (i.e., the terminal velocity). Understanding the rising velocity (i.e., terminal velocity) of the oil droplet plays a crucial role in determining the efficiency of the oil-water separation process systems. Therefore, good knowledge of the terminal velocity helps to optimize design and operating conditions.

Terminal velocity from CFD solvers was determined using the following equation:

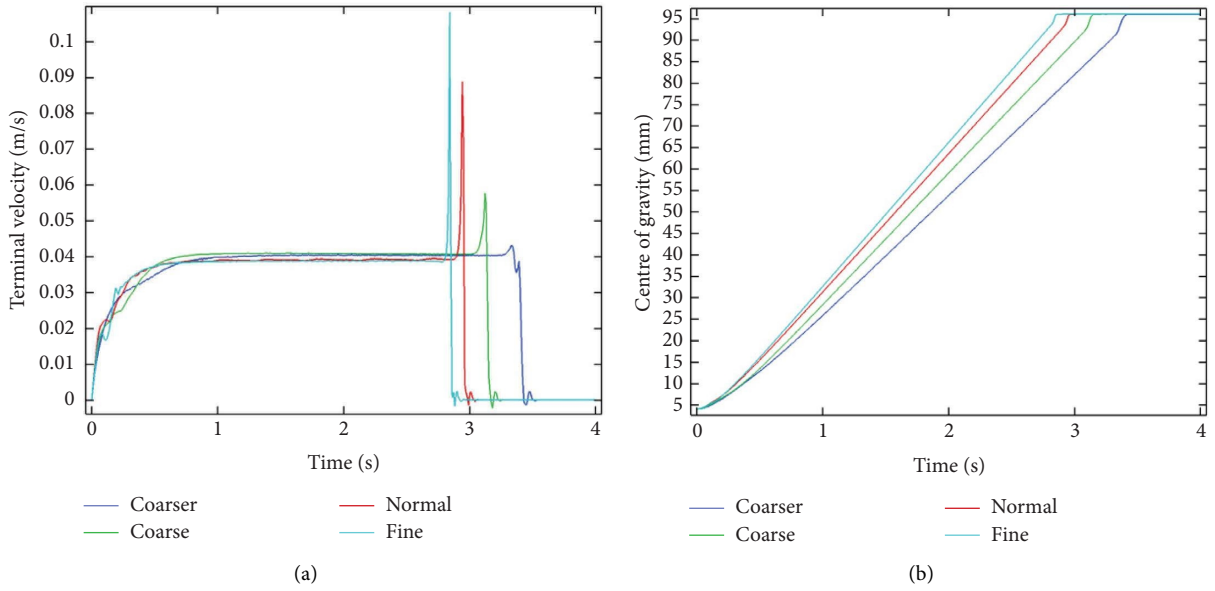

Figure 3: Motion of the oil droplet: (a) rising velocity versus time and (b) centre of gravity versus time.

Table 3: The average of the terminal velocity with different meshes.

Mesh type	Average terminal velocity (m/s)
Coarser	0.040241
Coarse	0.040918
Normal	0.039082
Fine	0.038751

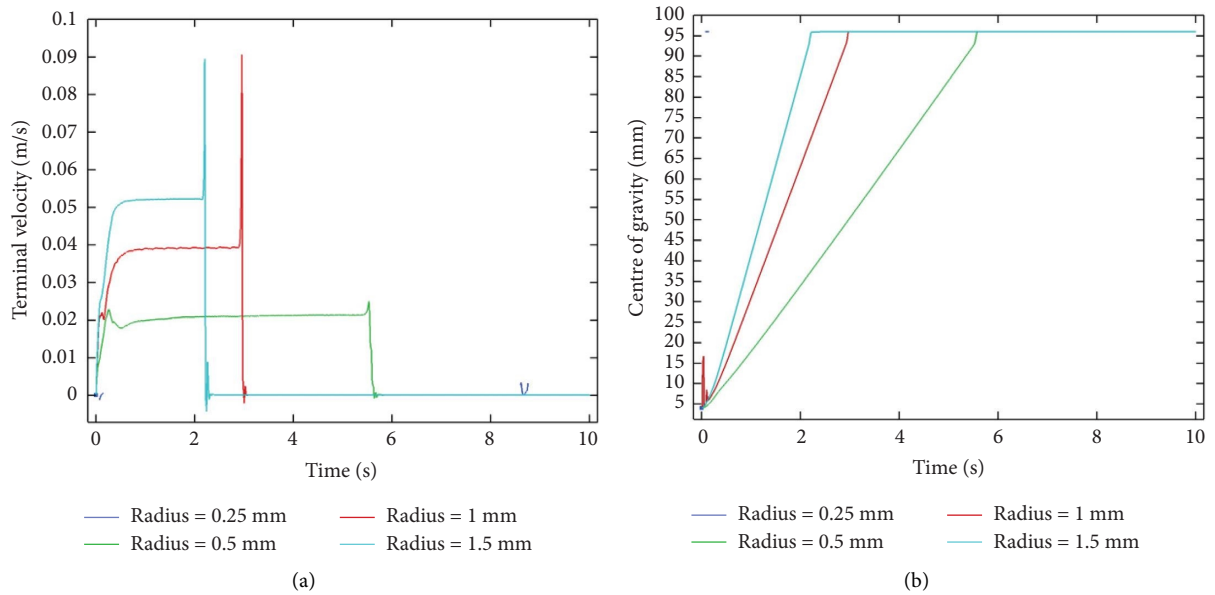

Figure 4: Motion of the oil droplet of Noor crude oil field: (a) rising velocity versus time and (b) centre of gravity versus time.

$$U_c = \left(\frac{\int_{\Omega_2} u \, dx}{\int_{\Omega_2} 1 \, dx} \right), \tag{17}$$

where Ω_2 denotes the region that occupied by the oil droplet.

The centre of gravity was used to monitor the translation of the oil droplet and it can be calculated using the following equation:

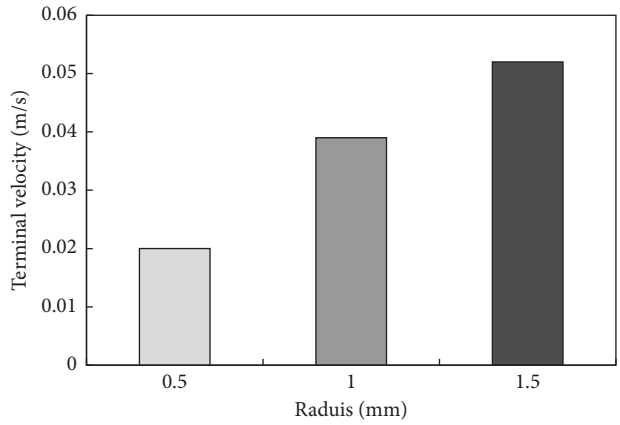

Figure 5: Terminal velocity versus the different crude oil droplet radius of the Noor crude oil field.

$$X_c = (x_c, y_c) = \left(\frac{\int_{\Omega_2} X dx}{\int_{\Omega_2} 1 dx} \right). \quad (18)$$

The available data of the crude oil properties from different oil fields in south of Iraq were used in this simulation (Table 1) [15]. The value of the interfacial tension between crude oil water $\sigma = 35$ (dyn/cm) was used [16].

2.3. The Mesh Resolution. To investigate the effect of mesh size (i.e., mesh resolution) on the simulation results, the following mesh types were used, which are coarser, coarse, normal and fine, as shown in Figure 2. The corresponding Grid numbers (i.e., statistics) are illustrated in Table 2.

3. Results and Discussion

3.1. The Effect of the Mesh Resolution. Figures 3(a) and 3(b) show the simulated results of the droplet terminal velocity and the centre of gravity. As it can be seen, the terminal velocities and the centre of gravity curves were very close when using normal and fine mesh grids, meanwhile the significant differences were observed with using the coarser and coarse meshes. Therefore, the grid resolution of the normal level was considered sufficiently high to represent the CFD simulation (i.e., it is selected based on the accurate results to reduce computational requirements).

In addition, to assess quantitatively the mesh-independent, the value of the average terminal velocity (the average of one hundred value) of the oil droplet of different meshes was determined (Table 3).

Table 3 shows that the average of the terminal velocities was close to each other especially with the normal and fine meshes (the percentage change is 0.846 %). This indicates that an unlikely significant change can be obtained in the average terminal velocity by using further mesh refinement. Therefore, the grid resolution of the normal level is considered sufficiently high to represent the CFD simulation (i.e., it is selected based on the accurate results to reduce computational requirements).

3.2. Effect of Oil Droplet Radius. Figure 4 shows the instantaneous velocity and centre of gravity versus the simulation time for different oil droplets' diameter. As it can be seen, the rising velocity of the crude oil droplet increased with increasing the radius of the oil droplets from 0.5 mm to 1.5 mm of the droplet (Figure 5) as a result of increasing the buoyancy force, which is the upward force exerted by the continuous phase (i.e., water column) that opposes the weight of the crude oil droplet. As the volume of the crude oil droplet becomes larger (i.e., diameter of the oil droplet becomes bigger), the buoyancy force also increased proportionally since the buoyancy force depends on the volume of fluid displaced (volume of water). Therefore, a larger droplet will experience a greater upward buoyancy force [17]. This leads to a direct a contribution of increasing the terminal velocity of the crude oil droplet.

For the oil droplet radius 1 mm, the maximum velocity was 0.039 (m/s) in a second. Afterwards, there is no variation in velocity until the oily layer was reached after 3 seconds. It means that the instantaneous rise velocities are in a steady condition. Meanwhile, the maximum rising velocity of 1.5 mm radius of oil droplet reached around 0.052 (m/s) in one second. Then, the rising velocity stayed almost at the same value (i.e., the steady state value) until reached the oily layer. The terminal velocity (the average of one hundred values) of 0.039, 0.052 (m/s) was found as the terminal velocity for oil droplet radius 1 and 1.5 mm, respectively. The increase in the rising velocity was observed when the radius of the droplet increased from 1 to 1.5 mm; the rising velocity incremented by 1.3 times and the time to reach the oily layer was reduced by 0.8s. When the droplet radius was 0.5 mm, the maximum rising velocity was around 0.022855093 (m/s) and after that decreased slowly and then reached the steady state value (terminal velocity = 0.02 (m/s)) (Figure 4(a)). When the oil droplets were with radius 0.25 mm, there were undetected graphs to describe the rising velocity and the centre of gravity. This might be related to the mass conservation issues of oil droplet with time.

The mass per unit volume of oil droplet is plotted against the time to track the mass lost during the simulation (Figures 6(a), 6(b), 6(c) and 6(d))). A clear mass loss when

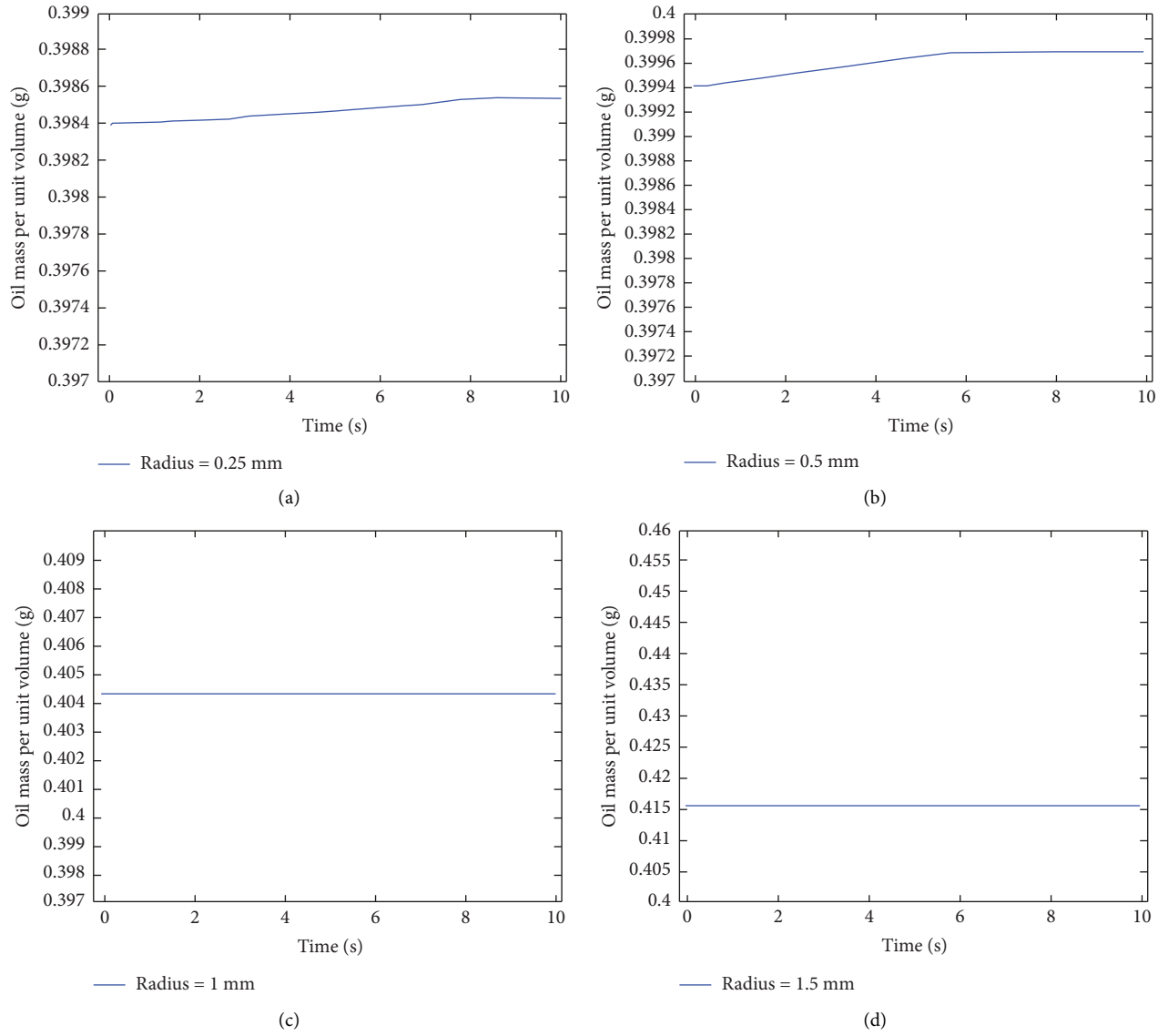

Figure 6: Oil mass per unit volume versus time of Noor crude oil field with (a) oil droplet radius 0.25 mm, (b) oil droplet radius 0.5 mm, (c) oil droplet radius 1 mm and (d) oil droplet radius 1.5 mm.

the radius of oil droplets was 0.25 mm and 0.5 mm (Figures 6(a) and 6(b)). This gives a reason why the terminal velocity was not stable for oil droplet with radius 0.5 mm (Figure 4(a)). In addition, the mass lost for the droplet with radius 0.25 mm led to disappear the droplet in the beginning time of the simulation; this is supported by the rising velocity contour (Figures 7(a) and 7(b))) and three-dimensional contour of the oil droplet (Figures 8(a) and 8(b)). Consequently, the CFD cannot deduct the terminal velocity and the centre of gravity (Figures 4(a), 4(b) and 5). However, the mass was constant (Figures 6(c) and 6(d)) when the radius was 1 mm and 1.5 mm, leading to give a correct curves to calculate the terminal velocity and the centre of gravity (Figures 4(a) and 4(b)). This is also supported by the rising velocity contour (Figures 7(c) and 7(d)) and three-dimensional contour of the oil droplet (Figures 8(c) and 8(d))

3.3. Effect of the S.G. To assess the effect of S.G. on the terminal velocity of the oil droplet, available data [15] of different crude oil field properties were used in simulation as illustrated in Table 1. It can be seen from Figures 9(a) and 9(b) that the rising velocity and the centre of gravity increased with decreasing the specific gravity. The main reason was related to the increase in the driving force ($\rho_{\text{water}} - \rho_{\text{crude oil}}$) that has a linear relationship with the rising velocity (equation (6)). The highest terminal velocity was found for Abu-Garab oil field (*S.G.* = 0.858, Terminal velocity = 0.044654 (m/s) (the evarage of 100 values)), whereas the lowest terminal velocity value was found for Hailfaya oil field (*S.G.* = 0.913, *Terminal velocity* = 0.029613 (m/s) (the evarage of 100 values)) (Table 4). Generally, the rising velocity can be increased significantly with decreasing the specific gravity (Figure 10). This leads to a decrease in the moving time to reach the upper layer (this is supported by

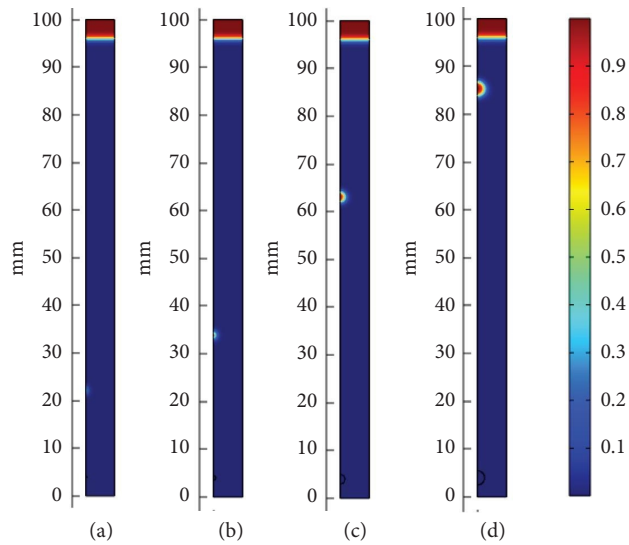

Figure 7: The magnitude of the velocity vector with different oil droplet radius (Noor crude oil field): (a) oil droplet radius 0.25 mm, (b) oil droplet radius 0.5 mm, (c) oil droplet radius 1 mm and (d) oil droplet radius 1.5 mm.

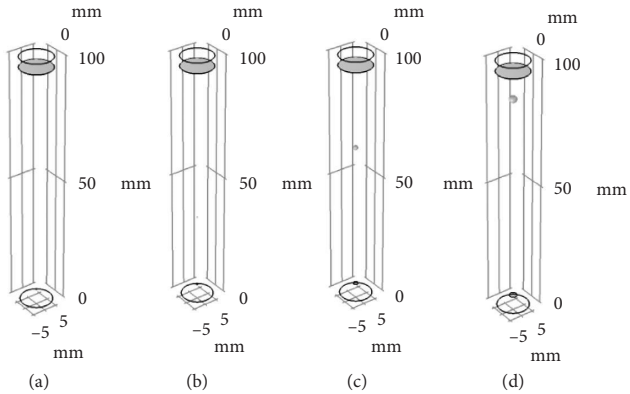

Figure 8: Three-dimensional contour of the oil droplet rising with different radius after 2 s (Noor crude oil field): (a) oil droplet radius 0.25 mm, (b) oil droplet radius 0.5 mm, (c) oil droplet radius 1 mm and (d) oil droplet radius 1.5 mm.

Figures 9 and 11) in the API separator unit and consequently enhancing the total separation process. The same situation can be found for the centre of gravity where the droplet moves faster with a reduction in the specific gravity of the crude oil. Although the specific gravity of the crude oil from Noor crude oil field was lighter than Faqa 2, the terminal velocity of Faqa 2 was faster than Noor. This was directly related to the value of viscosity (Figure 12), while the viscosity value of Noor crude oil was 40.1 cst, the viscosity value of Faqa 2 was 33.6 cst. According to equation (7), the drag coefficient improved with increasing the viscosity value, leading to an increase in the drag force that directly reduces the movement of the oil droplet (equation (6)).

3.4. Effect of Oil Droplet's Position. To investigate the effect of the oil droplet location (the height of the droplet from the bottom of the water column) on the dynamic properties of the oil droplet, four different positions were used as follows: (0, 4 mm), (0, 10 mm), (0, 30 mm) and (0, 60 mm). It is clear to see from Figures 13(a) and 13(b) that the same trends were found in terms of the terminal velocity and the centre of gravity for all different positions. However, there were small differences between the positions (Figure 14). Generally, the terminal velocity rose with the decrease in the height of water column over the oil droplet as it clears in Table 5.

3.5. Sudden Velocity Increment Phenomena. It is important to note that for all parameters and conditions used in this CFD simulation, at a certain time as the crude oil droplet, approach and meet the top layer (i.e., the oily layer). The terminal velocity of the droplet suddenly jumps to the maximum value and then the velocity rapidly decreases to zero (Figure 15). Such a phenomenon might be due to the fact that the value of the interfacial tension of crude oil droplet-water layer is typically higher than the value of crude oil droplet-crude oil layer. This leads to reduce the resistance

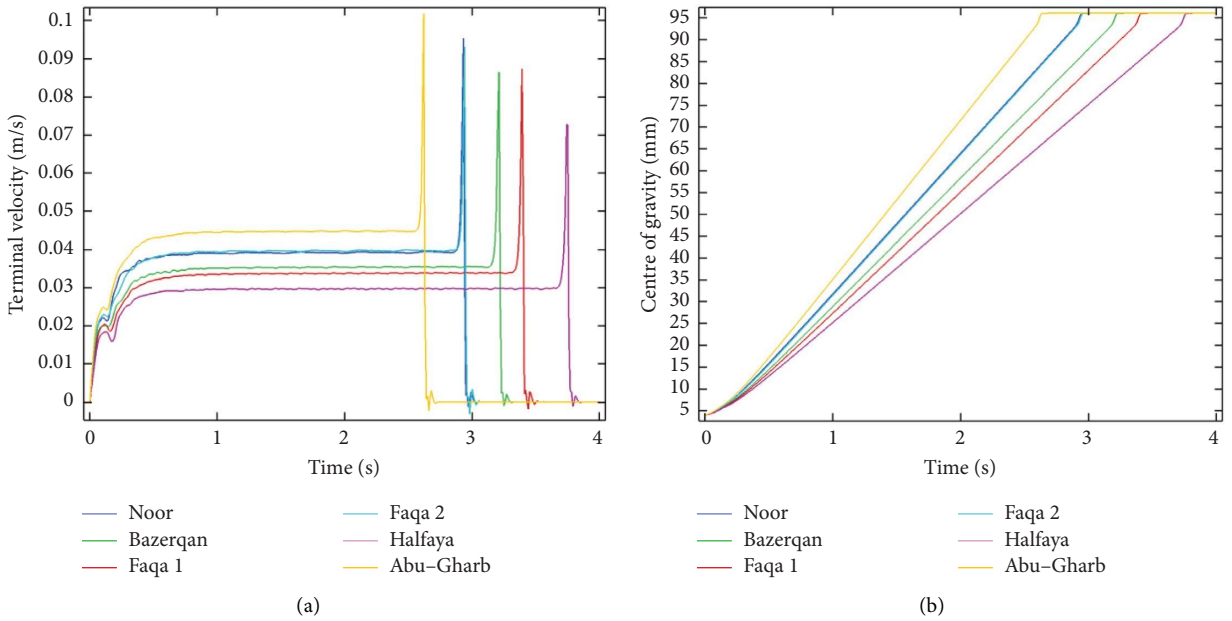

Figure 9: Motion of the oil droplet with radius = 1 mm: (a) rising velocity versus time and (b) centre of gravity versus time.

Table 4: Terminal velocity of different crude oil.

	Noor	Bazerqan	Faqa 1	Faqa 2	Hailfaya	Abu-Garab
Terminal velocity (m/s)	0.039072	0.035238	0.033647	0.039567	0.029613	0.044654

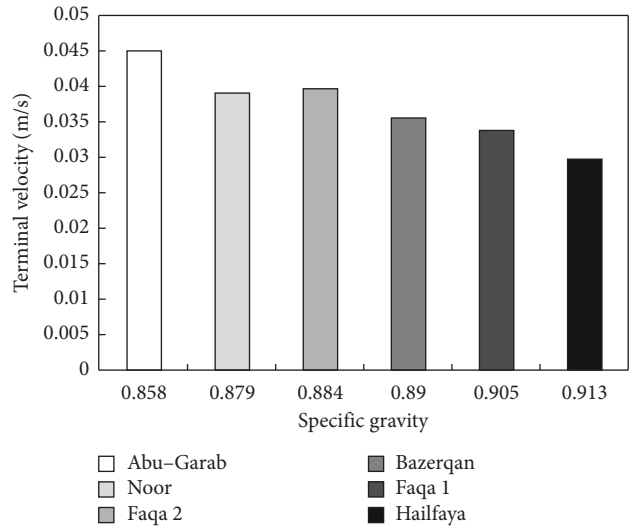

Figure 10: Terminal velocity versus the specific gravity of different crude oil with radius = 1 mm.

that faces the oil droplet. Consequently, with less resistance at the interface of crude oil droplet and crude oil layer, the droplet accelerates quickly leading to a sudden increment of the terminal velocity. After a while, the coalescence process (i.e., oil droplet coalesces with the oily layer) was occurred and led to a reduction in the velocity to zero (Figure 16).

3.6. Validation of Results. There is a need to validate the CFD results via experimental or simulation studies. Most of the literature focuses on studying the effect of the properties of the continuous phase (water), e.g., viscosity, salinity, pH and surface tension (surfactant addition) on the rising velocity and deformation shape of the oil droplet. However, the

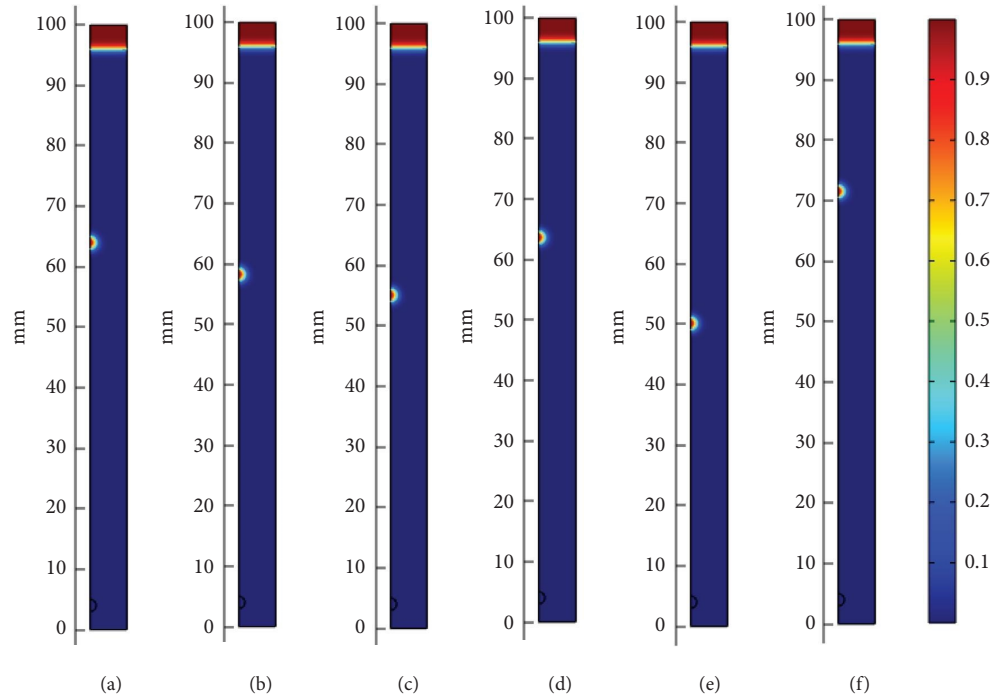

FIGURE 11: The magnitude of the velocity vector of the oil droplet (after 2 s) with different crude oils, with radius = 1 mm: (a) Noor, (b) Bazerqan, (c) Faqa 1, (d) Faqa 2, (e) Hailfaya and (f) Abu-Garab.

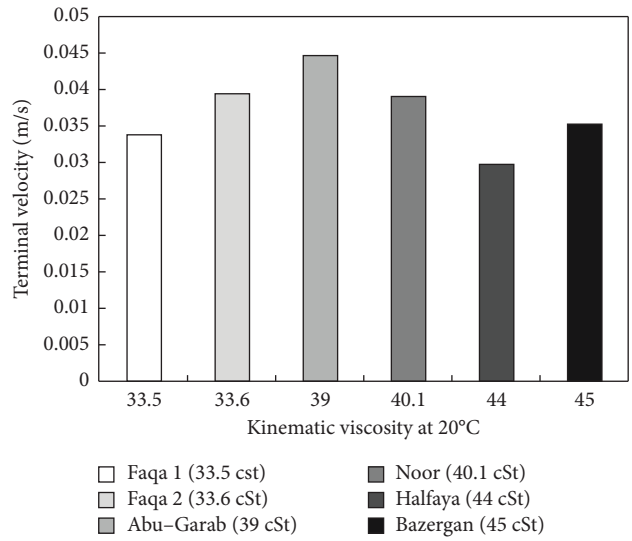

FIGURE 12: Terminal velocity versus the kinematic viscosity cSt of different crude oil with radius = 1 mm.

results of the current study were consistent with the same trend of the study conducted by Peters et al. [18], who used three different silicon oils with different properties (density and viscosity) to measure the rising velocity of the silicon oil droplet at constant temperature. They investigated the rising velocity versus a range of oil diameter from 0.5 to 9 mm. Based on their results, it can be concluded that the rising velocity increased by decreasing the oil density as a result of increasing the driving force $(\rho_o - \rho_w)$ and simultaneously decreased by increasing oil viscosity. Meanwhile, the rising velocity increased by increasing the oil droplet diameter. Moreover, the trajectory adopted by the oil droplets in different circumstances, in terms of specific gravity, viscosity, different radius and position, during the CFD

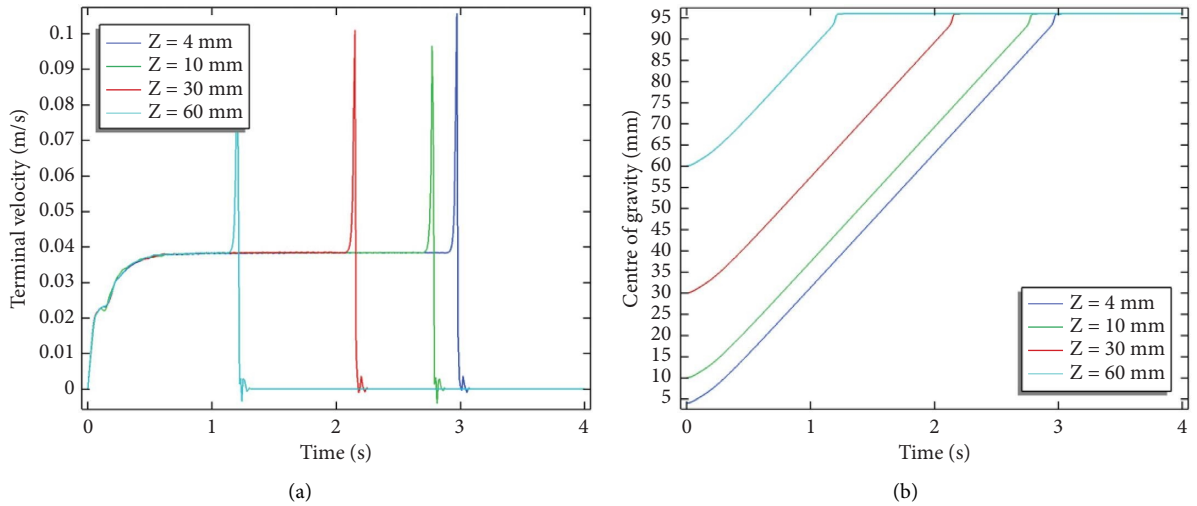

FIGURE 13: Motion of the oil droplet from Noor crude oil field with radius = 1 mm: (a) rising velocity versus time and (b) centre of gravity versus time.

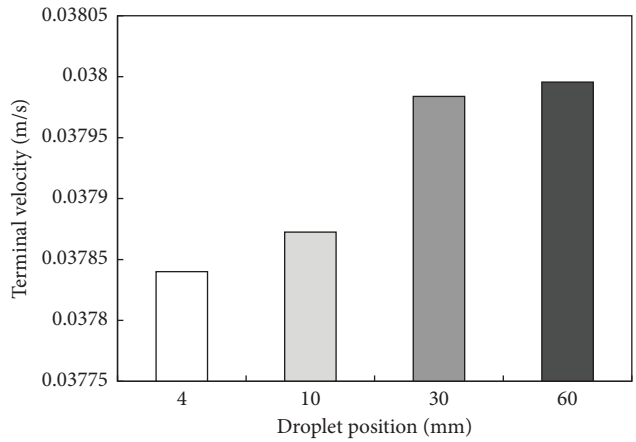

FIGURE 14: Terminal velocity versus the oil droplet's position (Noor crude oil field with radius = 1 mm).

TABLE 5: Terminal velocity of oil droplet for different positions.

	$Z = 4$ mm	$Z = 10$ mm	$Z = 30$ mm	$Z = 60$ mm
Terminal velocity (m/s)	0.037847	0.037872457	0.0379838051	0.037995562

simulation, was rectilinear path. These findings align with observations of an experimental and numerical study conducted by Rao et al. [7], who found that the droplets with diameter less than 5 mm moved in a linear path. To validate the value of the rising velocity of the oil droplet in this CFD simulation, the rising velocity was compared with simulation results (using ANSYS FLUENT) conducted by Gao et al. [9], who calculated the rising velocity of oil droplet with a diameter of 1 mm. The velocity was reported to be 0.032 (m/s); hence, it does not fit well with the CFD result of this study where the rising velocity of 1 mm oil droplet diameter was 0.039 (m/s). Although there is a small discrepancy between the two readings, this might be related directly to the value of the interfacial tension which plays a crucial role in the deformation of the oil droplet shape [19]) used in the studies. The present CFD simulation study applied an interfacial tension of 0.035 N/m that led to forming a spherical oil droplet shape and reduced the drag force which consequently gave rise to a higher terminal velocity. On the other hand, a lower interfacial tension of

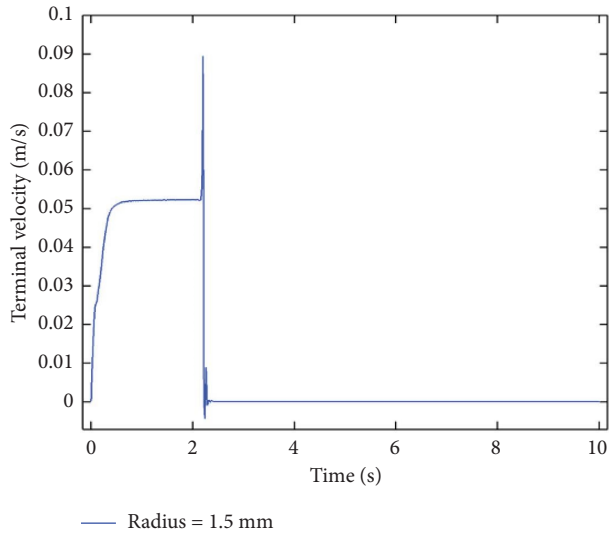

Figure 15: Rising velocity of crude oil droplet (Noor crude oil field radius = 1.5 mm) versus time.

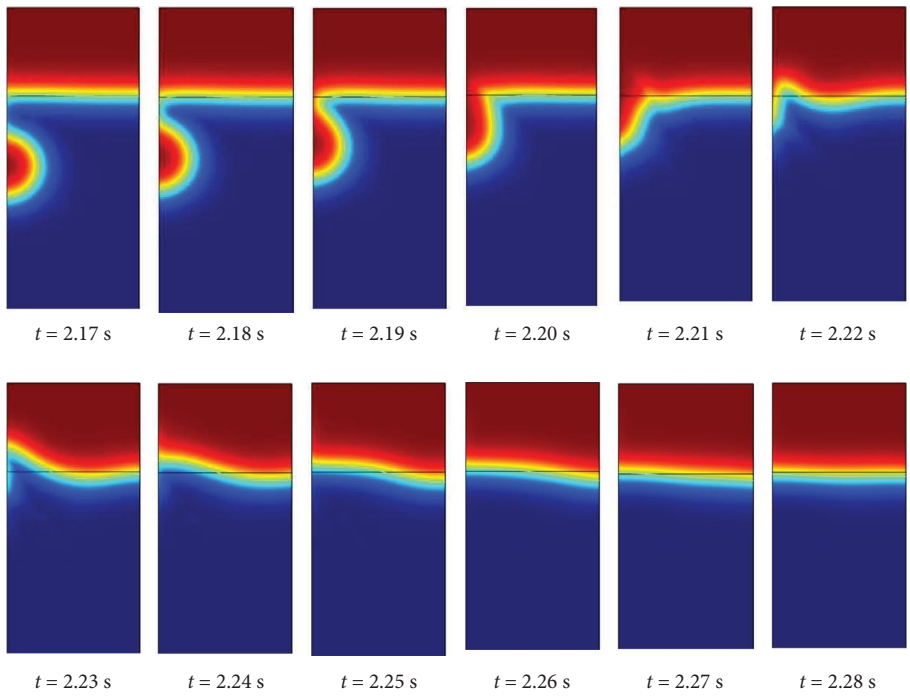

Figure 16: Steps of coalescence process of the oil droplet (Noor crude oil, oil droplet radius = 1.5 mm) with the oily layer as function of time.

0.022 N/m was used in the literature, contributing to deform the droplet shape and increase drag force, which in turn led to reducing the rising velocity.

4. Conclusions

To explore the impact of the type of the crude oil (i.e., specific gravity), oil droplet diameter and the oil droplet position on the dynamic motion of the oil droplet rising in an API oil–water separator, a CFD simulation was carried out using COMSOL Multiphysics by employing the level set model interface for two phases flow of crude oil droplet in a stagnant water column. Generally, the CFD simulation results indicated that the terminal velocity and the centre of the gravity were directly increased with decreasing the specific gravity. This was related to the increase in the driving force (i.e., the difference in the densities of the continuous phase and the crude oil droplet), that has a linear relationship with the rising velocity. While the highest terminal velocity was found for Abu-Garab oil field (*S.G.* = 0.858), the lowest terminal velocity value was found for Hailfaya oil field (*S.G.* = 0.913). In addition, by changing the radius of crude oil droplet from 1 mm to 3 mm the rising velocity showed an increase around 1.5 times. However, the

CFD simulation cannot be able to detect the terminal velocity when the radius of the droplet was 0.5 mm. Moreover, there was an increase in terms of the terminal velocity of the droplet as a result of decreasing the height of water column over the oil droplet.

CFD simulation exhibited a strong capability to visualize the hydrodynamic flow of the oil droplet in a stagnant aqueous phase in precise detail. Nonetheless, there is a need to validate the CFD outcomes with experimental studies, as none has been found, to the best of our knowledge, as most of the literature focuses on studying the properties of the continuous phase (water), e.g., viscosity, salinity, PH and surface tension. Therefore, the next work will be an experimental study to investigate the dynamic characteristics of crude oil droplet.

Data Availability Statement

The data that support the findings of this study are available from the corresponding author upon reasonable request.

Conflicts of Interest

The authors declare no conflicts of interest.

Funding

No funding was received for this research.

References

[1] F. B. P. da Silva Almeida, K. P. S. O. R. Esquerre, J. I. Soletti, and C. E. De Farias Silva, "Coalescence Process to Treat Produced Water: An Updated Overview and Environmental Outlook," *Environmental Science and Pollution Research* 26, no. 28 (2019): 28668–28688, https://doi.org/10.1007/s11356-019-06016-x.

[2] B. Cerff, D. Key, and B. Bladergroen, "A Review of the Processes Associated With the Removal of Oil in Water Pollution," *Sustainability* 13, no. 22 (2021): 12339, https://doi.org/10.3390/su132212339.

[3] D. Dardor, M. Al-Maas, J Minier-Matar, et al., "Protocol for Preparing Synthetic Solutions Mimicking Produced Water From Oil and Gas Operations," *ACS Omega* 6, no. 10 (2021): 6881–6892, https://doi.org/10.1021/acsomega.0c06065.

[4] A. A. Olajire, "Recent Advances on the Treatment Technology of Oil and Gas Produced Water for Sustainable Energy Industry-Mechanistic Aspects and Process Chemistry Perspectives," *Chemical Engineering Journal Advances* 4 (2020): 100049, https://doi.org/10.1016/j.ceja.2020.100049.

[5] X.-H. Liao, S. J. Yang, M. W Qin, et al., "Overview of Oil-Water Separation Equipment Technology of Refined Oil," *IOP Conference Series: Earth and Environmental Science* 508, no. 1 (2020): 012131, https://doi.org/10.1088/1755-1315/508/1/012131.

[6] C. Deng, W. Huang, H. Wang, S. Cheng, X. He, and B. Xu, "Preparation of Micron-Sized Droplets and Their Hydrodynamic Behavior in Quiescent Water," *Brazilian Journal of Chemical Engineering* 35, no. 2 (2018): 709–720, https://doi.org/10.1590/0104-6632.20180352s20160659.

[7] A. Rao, R. K. Reddy, F Ehrenhauser, et al., "Effect of Surfactant on the Dynamics of a Crude Oil Droplet in Water Column: Experimental and Numerical Investigation," *Canadian Journal of Chemical Engineering* 92, no. 12 (2014): 2098–2114, https://doi.org/10.1002/cjce.22074.

[8] L. Aprin, F. Heymes, P. Lauret, P. Slangen, and S. Le Floch, "Experimental Characterization of the Influence of Dispersant Addition on Rising Oil Droplets in Water Column," *Chemical Engineering Transactions* 43 (2015): 2287–2292.

[9] F. Gao, F. Cui, L. Zhao, and M. Boufadel, "Numerical Modeling of the Effect of Chemical Dispersant on Oil Droplet," in *ASTFE Digital Library* (Begel House Inc, 2019).

[10] M. A. Z. Zameek, M. W. Lim, and E. V. Lau, "Terminal Velocity of Heavy Crude Oil in Aqueous Solution: Effects of pH and Salinity," *International Proceedings of Chemical, Biological and Environmental Engineering* 96 (2016): 46–52, https://doi.org/10.7763/ipcbee.2016.v96.8.

[11] E. AlMatroushi and M. T. Ghannam, *Flow Behavior of Crude Oil Droplet Moving within Aqueous Solutions* (2011).

[12] B. Gopalan and J. Katz, "Turbulent Shearing of Crude Oil Mixed with Dispersants Generates Long Microthreads and Microdroplets," *Physical Review Letters* 104, no. 5 (2010): 054501, https://doi.org/10.1103/physrevlett.104.054501.

[13] K. Zhang, Y. Li, Q. Chen, and P. Lin, "Numerical Study on the Rising Motion of Bubbles Near the Wall," *Applied Sciences* 11, no. 22 (2021): 10918, https://doi.org/10.3390/app112210918.

[14] "Rising Bubble," https://www.comsol.com/model/rising-bubble-177.

[15] H. Hadi Jasim and R. Abd Al-Hussain, "Evaluation of Inhibitor Efficiency in Crude Oil Pipeline of Missan Oil Fields South Iraq," *Journal of Engineering and Sustainable Development* 23, no. 01 (2019): 145–161, https://doi.org/10.31272/jeasd.23.1.11.

[16] "Capillary Pressure," https://wiki.aapg.org/Capillary_pressure.

[17] A. Rosikhin, E. Sulistio, D. R. Sofia, and F. Faizal, "Effect of Bubble Size on the Rising Behavior in Pure Water Medium," *Journal of Physics: Conference Series* 2344, no. 1 (2022): 012015, https://doi.org/10.1088/1742-6596/2344/1/012015.

[18] F. Peters, M. Nüllig, and D. Miletic, "Rise of Oil Drops in Water and Fall of Water Drops in Oil," *Forschung im Ingenieurwesen* 78, no. 3-4 (2014): 87–91, https://doi.org/10.1007/s10010-014-0176-8.

[19] F. Peters and D. Arabali, "Interfacial Tension between Oil and Water Measured with a Modified Contour Method," *Colloids and Surfaces A: Physicochemical and Engineering Aspects* 426 (2013): 1–5, https://doi.org/10.1016/j.colsurfa.2013.03.010.